

Embrittlement of Austenitic Stainless Steel Welds

S. A. David, J. M. Vitek, and D. J. Alexander¹

Received March 27, 1995; revised May 14, 1996

To prevent hot-cracking, austenitic stainless steel welds generally contain a small percent of delta ferrite. Although ferrite has been found to effectively prevent hot-cracking, it can lead to embrittlement of welds when exposed to elevated temperatures. The aging behavior of type-308 stainless steel weld has been examined over a range of temperatures 400–850°C for times up to 10,000 hr. Upon aging, and depending on the temperature range, the unstable ferrite may undergo a variety of solid state transformations. These phase changes affect creep-rupture and Charpy impact properties.

KEY WORDS: Austenite; austenitic stainless steel; carbides; creep; embrittlement; ferrite; fracture toughness; sigma phase; and welds.

1. INTRODUCTION

Austenitic stainless steels are widely used in several industries such as power generation (both conventional and nuclear) and chemical and petrochemical industries because of their excellent corrosion resistance as well as their good mechanical properties. Fully austenitic stainless steel welds are prone to hot-cracking during welding. Several studies have shown that a certain amount of delta ferrite (δ) phase should be present in the welds to prevent hot-cracking.^(1–3) Therefore, austenitic stainless steel welds normally contain 5–10% ferrite. The origin of ferrite and the role of ferrite in preventing hot-cracking has been addressed elsewhere.^(1–7) The ferrite phase in austenitic stainless steel welds has been found to exist in four distinct types of morphologies, namely vermicular, lacy, acicular, and globular.⁽⁸⁾ Although ferrite in austenitic stainless steel welds has a beneficial effect in preventing hot-cracking during welding, when exposed to elevated temperatures during service, the duplex structure of austenite (γ) + ferrite (δ) embrittles extensively, leading to a degradation in the mechanical behavior of the weld metal.

The paper describes this embrittlement in type-308 austenitic stainless steel welds over a range of temperatures. Typical composition of the weld is Cr-20.2, Ni-9.4, Mn-1.7, Si-0.5, C-0.05, N-0.06 balance Fe (in wt. %).

2. WELD METAL MICROSTRUCTURE

A typical microstructure of type-308 austenitic stainless steel weld metal containing γ and δ ferrite is shown in Fig. 1. The origin of this microstructure is due to the nonequilibrium nature of the transformations that follow weld pool solidification and subsequent cooling of the weld metal to room temperature. Figure 2 shows a vertical section of the iron-chromium-nickel ternary phase diagram showing the location of a typical type 308 stainless steel composition. An earlier study⁽⁴⁾ revealed the solidification sequence in type 308 stainless steel weld metal, consisting of the primary crystallization of δ -ferrite with subsequent envelopment of δ -ferrite by austenite and a $\delta \rightarrow \gamma$ transformation continuing below the solidus. The result is a skeletal network of residual ferrite. This particular ferrite has been shown to be located along the cores of the primary and secondary dendrite arms and is enriched in chromium (Fig. 3).

¹ Metals and Ceramics Division, Oak Ridge National Laboratory, Oak Ridge, Tennessee 37831-6095.



Fig. 1. Typical as welded microstructure of type 308 stainless steel.

Sometimes the primary δ -ferrite that formed during solidification may transform to Widmanstätten austenite at lower temperatures, leaving behind residual ferrite in the acicular or lacy forms. Other investigations by Suutala *et al.*⁽⁵⁾ and Takalo *et al.*⁽⁶⁾ have clearly identified the mode of freezing and the resulting microstructures of austenitic stainless steel welds as a function of Cr/Ni equivalent ratios. Ferrite and austenite are the major phase constituents in the austenitic stainless steel welds. In addition, stainless steels contain small amounts of carbon (0.05 wt. %) which promotes carbide precipitation upon aging.

3. AGING BEHAVIOR OF AUSTENITIC STAINLESS STEEL WELDS

3.1. Aging at Temperatures $\geq 550^\circ\text{C}$

Upon aging the welds at temperatures 550, 650, 750, 850°C for times up to 10,000 hr, a number of changes in the as-welded microstructures were observed.^(9,10) During the early stages of aging, at the original austenite/ferrite interface, precipitation of $M_{23}C_6$ carbide with a cube-on-cube orientation relationship

with the austenite matrix was found (Fig. 4). At the same time, the ferrite was found to dissolve to a limited extent, leaving the residual ferrite more enriched in chromium and depleted in nickel. Upon aging further, ferrite transformed to sigma phase. Figure 5 reveals the structure after 100 hr aging wherein the original austenite/ferrite boundary is clearly marked by the $M_{23}C_6$ precipitates and the ferrite has transformed to sigma phase. In the electron micrograph, the receded ferrite boundary due to the dissolution of ferrite can also be seen. The continuous network of the carbides could result in a degradation of the mechanical properties of the weld metal.

Partial transformation of ferrite to sigma phase was rarely observed. Islands were typically found to be all ferrite or all sigma. However, some ferrite islands were found to remain untransformed even after aging for up to 10,000 hr at 650°C. These ferrite regions were substantially enriched in chromium, with levels nearly identical to those found in sigma phase. These observations indicate that the nucleation of sigma phase in ferrite is the rate limiting step for the transformation.⁽¹⁰⁾ They indicate that although the chromium enrichment of ferrite is a necessary step, it is not sufficient for sigma formation. Also, the fact that partially transformed ferrite areas were rarely observed indicates that once nucleation of

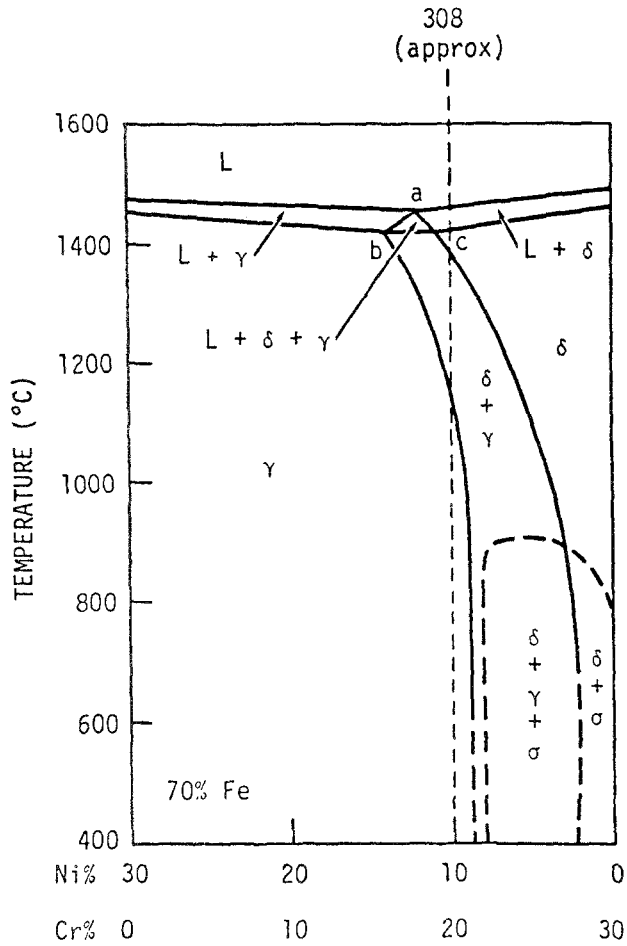


Fig. 2. Vertical section of the Fe-Cr-Ni ternary phase diagram at 70 wt. % iron. The dashed line represents the approximate composition of type 308 stainless steel.

sigma phase begins, the subsequent growth of sigma is relatively fast.

A composite of typical energy dispersive X-ray spectra of the four phases, namely, austenite, ferrite, sigma, and $M_{23}C_6$ is shown in Fig. 6. A comparison of the relative peak heights of chromium and iron clearly shows an increase in chromium content for the order of phases given above. A comparison of the nickel to iron peak height shows that nickel is substantially higher in austenite. Typical normalized iron, chromium, and nickel compositions of these phases are (in wt. %): 69-Fe, 23-Cr, 8-Ni, (austenite); 68-Fe, 28-Cr, 4-Ni (ferrite); 59-Fe, 38-Cr, 3-Ni (sigma); and 17-Fe, 79-Cr, 4-Ni (carbide).

Although most of the above discussions pertain to aging of the welds at 650°C, the sequences of events that follow aging of the welds at 550°C, 750°C, and 850°C have been found to be the same as above. How-

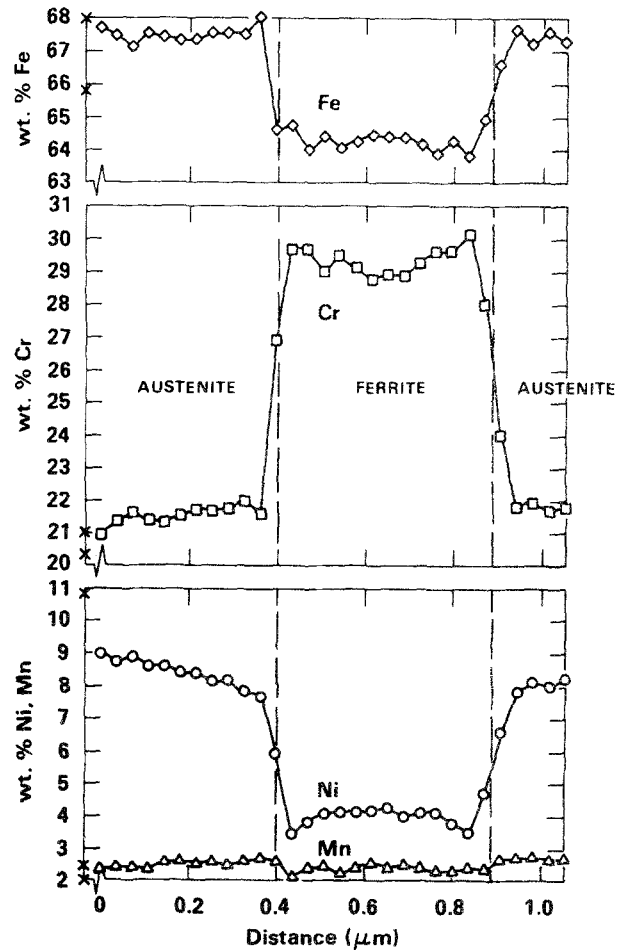
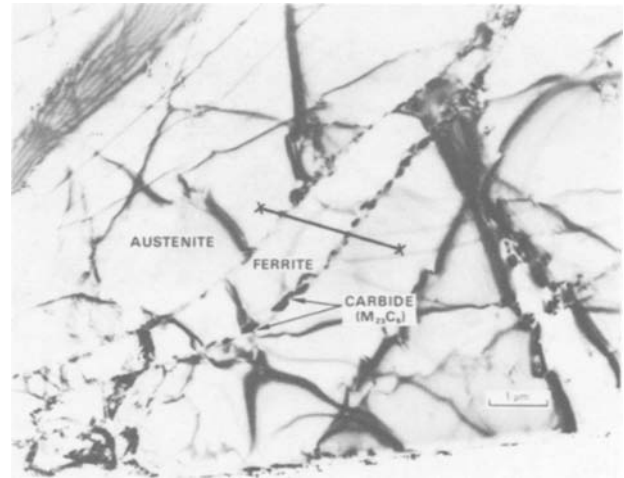


Fig. 3. Electron micrograph showing the ferrite area scanned to produce the composition profile across ferrite in the as-welded condition and the iron, nickel, chromium, and manganese profiles across the ferrite.

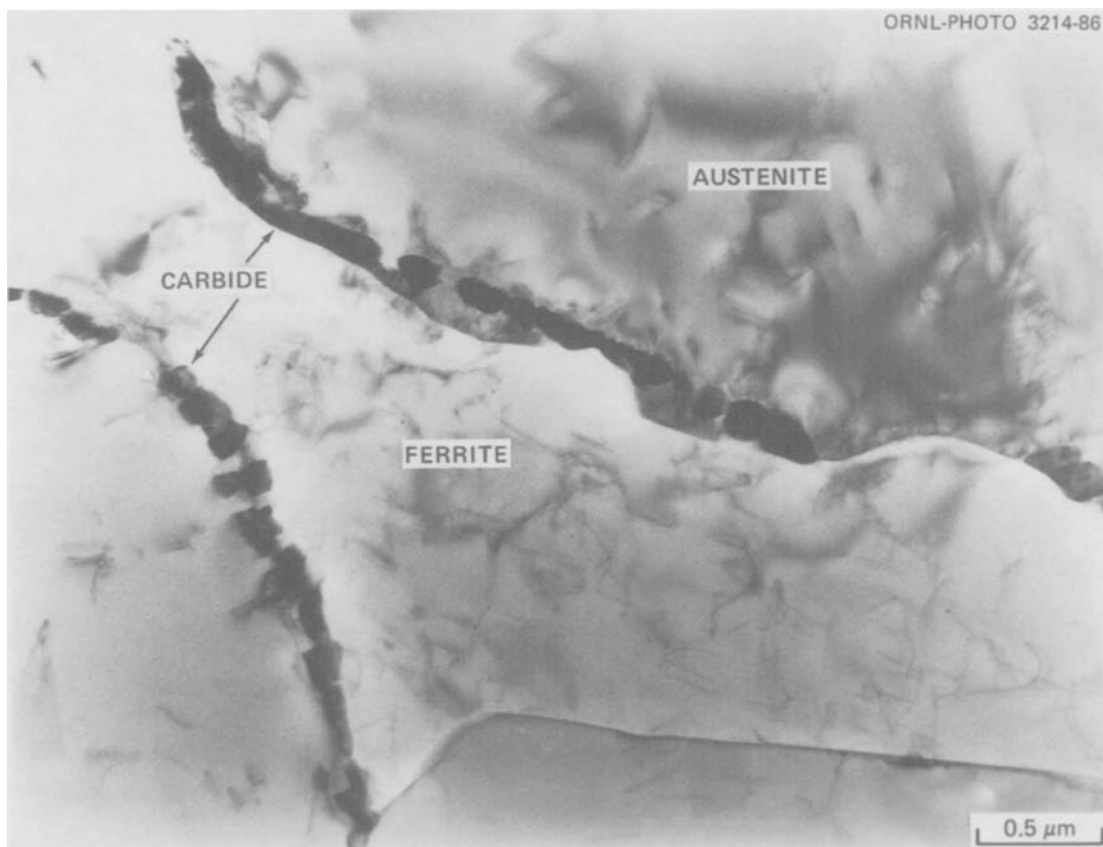


Fig. 4. Electron micrograph of type 308 stainless steel weld aged at 650°C for 18 min.

ever the kinetics of these phase reactions at 750°C and 850°C are much faster than that observed at 650°C, and they are considerably slower at 550°C.

Of the various phase changes that follow aging of type 308 stainless steel welds at temperatures greater than 550°C, the most damaging for weld-metal creep properties is the formation of an $M_{23}C_6$ carbide network. Creep testing of type 308 stainless steel welds at elevated temperatures has revealed extensive degradation in creep rupture properties including loss of creep ductility.^(9,11) Studies in this area have clearly identified the continuous network of $M_{23}C_6$ carbide in the weld to be the main cause for the degradation in creep rupture properties.⁽¹¹⁾ An examination of the creep rupture specimens revealed extensive creep void formation at the $M_{23}C_6/\gamma$ interface and also interconnecting tears along this interface. A dramatic improvement in creep rupture properties of the austenitic stainless steel welds can be achieved by the addition of controlled residual elements (CRE).^(12,13) These are additions of small amounts of 0.5–0.6 wt. % titanium and 50–60 ppm of boron. With the titanium additions, the improvement in creep rupture

properties of type 308 stainless steel welds is associated with the elimination of the continuous network of $M_{23}C_6$ carbides. The role of boron in improving the creep rupture properties of the weld is under investigation.⁽¹⁴⁾

3.2. Aging at Temperatures <550°C

Aging of type-308 stainless steel weld at 400°C or 475°C for times up to 5000 hr showed a number of changes in the as-welded microstructure. Unlike the specimens aged at temperatures greater than 550°C, aging at temperatures less than 550°C showed no evidence of ferrite-to-sigma phase transformation. However, $M_{23}C_6$ carbide precipitation at the austenite/ferrite interface was found to occur. During the initial stages of aging, within the ferrite, a fine-scale spinodal decomposition of ferrite into iron-rich α and chromium-rich α' phases was observed,^(15,16) as shown in Fig. 7. This decomposition of ferrite in the weld is similar to the observations made in some ferritic steels.^(17–22) This particular transformation has been found to embrittle the ferritic steel. Within the ferrite, in addition to the spi-

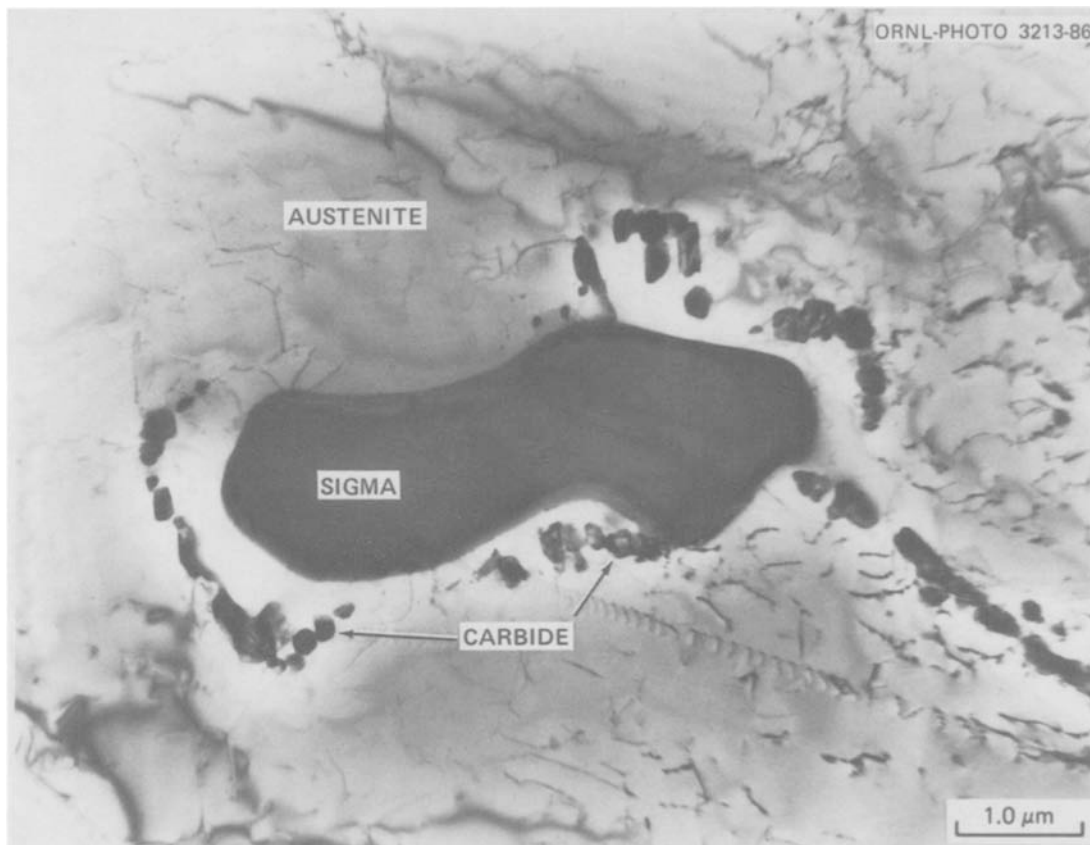


Fig. 5. Electron micrograph of type 308 stainless steel weld aged at 750°C for 100 hr.

nodal decomposition, abundant precipitation of G-phase was observed. G-phase is a nickel-rich silicide that has been identified in both austenitic stainless steel welds and castings.^(16,23-26) Microstructural changes observed in specimens aged at 400°C and 475°C were similar except the kinetics of the transformation were faster at 475°C.

Investigations were also carried out to correlate the microstructural development as a function of aging time and temperature with the degradation in mechanical properties such as tensile, impact and fracture toughness.⁽¹⁶⁻²⁷⁾ The results indicate extensive hardening of the ferrite during aging.⁽¹⁵⁾ Also during the early stages of aging, there is a shift in the Charpy impact ductile-brittle transition temperature (DBTT) as shown in Fig. 8. With extended aging, a drop in the upper-shelf energy was also observed. These observations can be attributed to the extensive solid-state transformations that occur within the ferrite during aging. The observed trend in Charpy impact properties was similar for specimens aged at 400°C and 475°C for times up to 5000 hr except that the specimens aged at 475°C showed a larger drop in the upper-shelf energy and a more rapid increase in

the DBTT with aging time. Although these observed changes in the impact properties can be attributed to the complex changes in the microstructural features that occur within and around the ferrite phase, the role of each transformation on the properties has not been identified. This is the goal of an ongoing investigation that is being carried out using experimental alloys.⁽²⁸⁾

3.3. Application of Nondestructive Examination (NDE)

When austenitic stainless steel welds are exposed to elevated temperatures, several phase changes take place as described above. It is likely that each of these phase changes has an adverse impact on mechanical behavior. Although the specific role of each of these transformations on embrittlement has not been identified, it would be desirable to be able to monitor these changes using NDE techniques. Unfortunately, the scale of many of these phase changes is very fine and beyond the limitations of current techniques. Hence, there is a critical

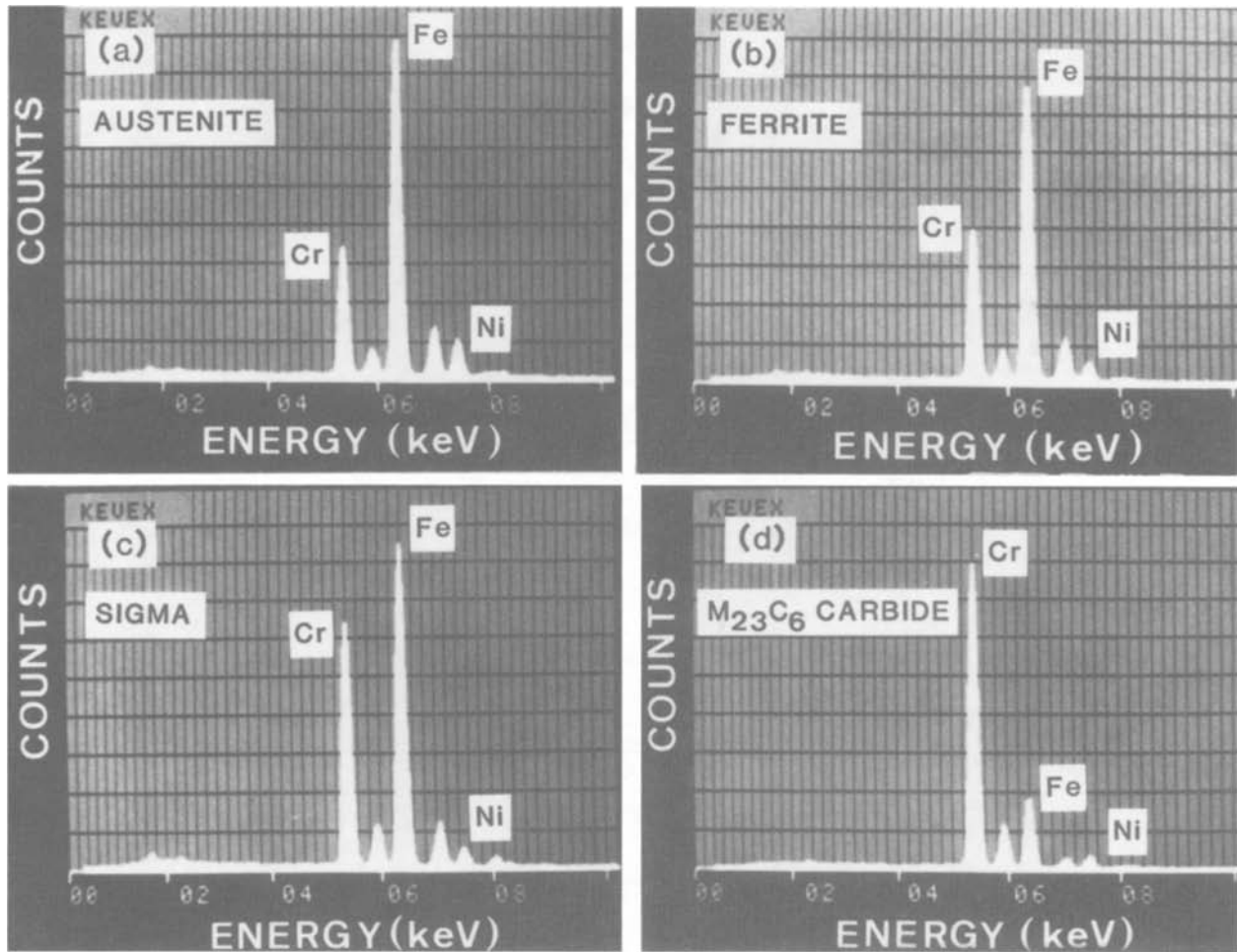


Fig. 6. Typical EDS spectra of phases found in aged type 308 stainless steel weld.

need to develop an appropriate NDE technique to monitor phases changes in materials on a microscopic scale.

4. SUMMARY

Exposure of austenitic stainless steel welds to elevated temperatures can lead to extensive changes in the microstructural features of the weld metal. The welds normally contain a duplex $\gamma + \delta$ microstructure. On exposure to elevated temperatures over a long period of time, a continuous network of $M_{23}C_6$ carbide forms at the austenite/ferrite interface. Often the network has been observed to be interconnected. The formation of the network of carbides has been found to reduce the elevated temperature creep-rupture properties of the type-308 stainless steel welds. The ferrite in type-308 austenitic stainless steel welds has been found to be un-

stable, and upon aging at temperatures between 550–850°C it transforms to sigma phase. All of these phase changes have been found to influence the creep-rupture properties of the weld metal. At temperatures below 550°C the ferrite has been found to decompose spinodally into α and α' phases. In addition, precipitation of G-phase occurs within the decomposed ferrite after low temperature aging. The decomposition of ferrite to α and α' phases increases the hardness of ferrite and, along with the precipitation of G-phase and carbides, leads to embrittlement of the weld metal as revealed by the Charpy impact properties.

ACKNOWLEDGMENTS

The authors would like to thank S. S. Babu and E. Ohriner for reviewing the manuscript. Research is spon-

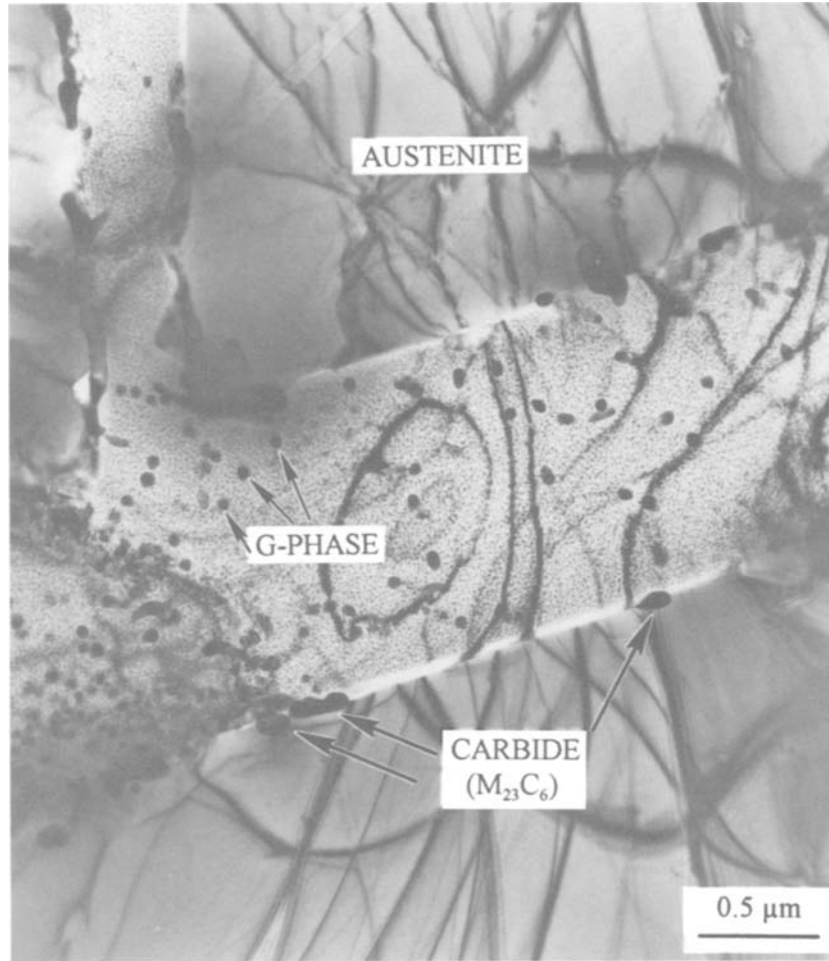


Fig. 7. Electron micrograph of decomposed ferrite in a weld aged at 475°C for 5000 hr. The electron micrograph shows the G-phase, $M_{23}C_6$ carbides, and the mottled nature of the spinodally decomposed ferrite into α and α' phases.

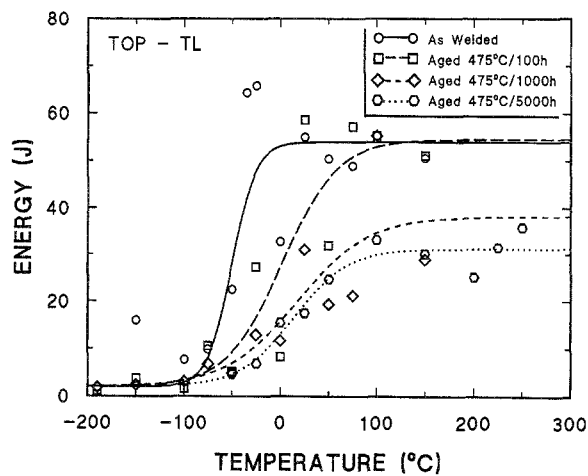


Fig. 8. Charpy impact test results (impact energy vs. test temperature) as a function of aging time at 475°C.

sored by the Division of Materials Sciences, U.S. Department of Energy, under contract DE-ACO5-96OR22464 with Lockheed Martin Energy Research Corporation.

REFERENCES

1. J. C. Borland and R. N. Younger, Some aspects of cracking in austenitic steels, *British-Welding J.* 7(1):22-60 (1960).
2. F. C. Hull, Effect of delta ferrite on the hot cracking of stainless steel, *Welding J.* 46(9):399-s-409-s (1961).
3. Y. Arata, F. Matsuda, and S. Katayama, Solidification crack susceptibility in weld metals of fully austenitic stainless steel (Report 1)—fundamental investigation on solidification behavior of fully austenitic and duplex microstructures and effect of ferrite on microsegregation, *Trans. Jpn. Welding Res. Ins.* 5(2):35-51 (1976).
4. S. A. David, G. M. Goodwin, and D. N. Braski, Solidification behavior of austenitic stainless steel filler metals, *Weld J.* 58(11): 330s-336s (1979).

5. N. Suutala, T. Takalo, and T. Moisiso, Relationship between solidification and microstructure in austenitic and austenitic-ferritic stainless steel welds, *Metall. Trans.* **10A**:512–514 (1979).
6. T. Takalo and T. Moisiso, Single phase ferritic solidification mode in austenitic-ferritic stainless steel welds, *Metall. Trans.* **10A**:1183–1190 (1979).
7. W. T. DeLong, Ferrite in austenitic stainless steel weld metal, *Welding J.* **53**(7):273-s–286-s (1974).
8. S. A. David, Ferrite morphology and variations in ferrite content in austenitic stainless steel welds, *Weld. J.* **60**(4):63s–71s (1981).
9. J. M. Vitek and S. A. David, The solidification and aging behavior of types 308 and 308CRE stainless steel welds, *Weld. J.* **63**:246s–253s (1984).
10. J. M. Vitek and S. A. David, The sigma phase transformation in austenitic stainless steel, *Weld. J.* **65**:106s–111s (1986).
11. J. M. Vitek, S. A. David, and V. K. Sikka, Examination of types 308 and 308CRE stainless steels after interrupted creep testing, *Weld. J.* **71**:421s–435s (1992).
12. R. T. King, J. O. Stiegler, and G. M. Goodwin, Relation between mechanical properties and microstructure in CRE type 308 weldments, *Weld. J.* **53**:307s–313s (1974).
13. J. O. Stiegler, R. T. King, and G. M. Goodwin, Effect of residual elements on fracture characteristics and creep ductility of type 308 stainless steel weld metal, *J. Eng. Mater. Technol.* **97**:245–250 (1975).
14. S. S. Babu, S. A. David, and J. M. Vitek, Work in progress (Oak Ridge National Laboratory, 1995).
15. S. A. David, J. M. Vitek, J. R. Keiser, and W. C. Oliver, Nanoindentation microhardness study of low-temperature ferrite decomposition in austenitic stainless steel welds, *Weld. J.* **66**:235s–240s (1987).
16. J. M. Vitek, S. A. David, D. J. Alexander, J. R. Keiser, and R. K. Nanstad, Low temperature aging behavior of type 308 stainless steel weld metal, *Acta Met. Mater.* **39**(4):503–516 (1991).
17. R. M. Fisher, E. J. Dulis, and K. G. Carroll, Identification of the precipitate accompanying 885°F embrittlement in chromium steels, *Trans. AIME* **197**:690–695 (1953).
18. R. O. Williams and H. W. Paxton, The nature of aging binary iron-chromium alloys around 500°C, *J. Iron Steel Inst.* **185**:358–374 (1957).
19. D. Chandra and L. H. Schwartz, Mossbauer effect study of the 475°C decomposition of Fe–Cr, *Metall. Trans. A.* **2A**:511–519 (1971).
20. J. Nishizawa, M. Hasebe, and M. Ko, Thermodynamic analysis of solubility and miscibility gap in ferromagnetic alpha iron alloys, *Acta Metall.* **27**:817–828 (1979).
21. T. J. Nichol, A. Dotta, and G. Aggun, Embrittlement of ferritic stainless steel, *Metall. Trans. A* **11A**:573–585 (1980).
22. S. S. Brenner, M. K. Miller, and W. A. Soffa, Spinodal decomposition of iron-32 at % chromium at 470°C, *Scripta Metall.* **16**:831–836 (1982).
23. J. M. Vitek, G-phase formation in aged type 308 stainless steel, *Metall. Trans. A.* **18A**:154–156 (1987).
24. H. M. Chung and O. K. Chopra, Kinetics and mechanism of thermal aging embrittlement of duplex stainless steels, in *Environmental Degradation of Materials in Nuclear Power Systems—Water Reactors*, G. J. Theus and J. R. Weeks, eds. (TMS-AIME, Warrendale, PA, 1988), p. 359.
25. M. K. Miller and J. Bentley, Characterization of fine-scale microstructures in aged primary coolant pipe steels, in *Environmental Degradation of Materials in Nuclear Power Systems—Water Reactors*, G. J. Theus and J. R. Weeks, eds. (TMS-AIME, Warrendale, PA, 1988), p. 341.
26. M. Vrinat, R. Cozar, and Y. Meyzaud, Precipitated phases in the ferrite of aged cast stainless steels, *Scr. Metall.* **20**:1101–1106 (1986).
27. D. J. Alexander, J. M. Vitek, and S. A. David, Long-term aging of type 308 stainless steel welds: Effects on properties and microstructure, in *International Trends in Welding Science and Technology*, S. A. David and J. M. Vitek, eds. (ASM-International, Materials Park, Ohio, 1993), p. 557.
28. J. M. Vitek, S. A. David, and D. J. Alexander, Oak Ridge National Laboratory, Oak Ridge, TN (1995).